Hindawi
Geofluids
Volume 2022, Article ID 4435881, 19 pages
https://doi.org/10.1155/2022/4435881

Research Article

Improvement of Steam Injection Efficiency in Horizontal Well with the Semi-Analytical Model: A Case Study of Liaohe Oilfield Steam Injection Well

He Zhang,[1] Xiaofeng Zhou ,[2,3] and Ao Zhang[4]

[1]*Daqing Oilfield Co., Ltd, Daqing 163458, China*
[2]*Key Laboratory of Continental Shale Hydrocarbon Accumulation and Efficient Development (Northeast Petroleum University), Ministry of Education, Northeast Petroleum University, Heilongjiang, Daqing 163318, China*
[3]*Institute of Unconventional Oil & Gas, Northeast Petroleum University, Daqing 163318, China*
[4]*School of Earth Sciences, Northeast Petroleum University, Heilongjiang, Daqing 163318, China*

Correspondence should be addressed to Xiaofeng Zhou; zhou_xiaofeng1993@163.com

Received 5 April 2022; Revised 2 May 2022; Accepted 6 May 2022; Published 25 May 2022

Academic Editor: Hao Wu

As China's largest heavy oil field, Liaohe oilfield encounters many problems after long-term thermal recovery, including high water percentage at early production stage, steam channelling and water cresting. To solve the above problems, the steam flow behavior and thermal characteristics in horizontal well should be understood. In this paper, a semi-analytical model is proposed to investigate the thermal properties and heat losses along the steam injection horizontal wellbore. The flow pattern is determined by the modified Beggs-Brill method and different conservation equations are incorporated to calculate the steam pressure, steam temperature and steam quality. The model shows good consistency with the field data of the horizontal steam injection well in Liaohe oilfield. The sensitivity analysis shows that the steam quality along the wellbore is strongly affected by the steam pressure, steam injection rate and steam quality at the heel. Generally, the steam injection rate does not have significant effect on steam pressure, steam temperature and steam quality. The model is then used to optimize the injection parameters of Well XH27 to improve the steam injection efficiency. After optimization, more steam is injected to the formation to heat the region near the wellbore, which leads to a higher production rate. In summary, this study presents a semi-analytical model to calculate the thermal properties of steam and the model can be used to optimize steam injection process for field application.

1. Introduction

As China's largest heavy oil production region, Liaohe oilfield has made significant achievements in the development of heavy and extra-heavy oil with thermal recovery technique using horizontal wells [1, 2]. After long-term production, thermal recovery in Liaohe oilfield encounters many problems: 1) emergence of steam/water during early development, 2) uneven use of horizontal sections, and 3) steam channelling or water cresting [3]. Recently, Liaohe oilfield has applied double-pipe or multi-point steam injection technique to avoid the problems brought by uniform steam injection. However, the fundamental problems of screen open-hole plugging, optimal steam injection volume and early emergence of steam/water remain unsolved [4]. It is of great necessity to find a new method to investigate the temperature and pressure distribution in horizontal wells and therefore improve the efficiency of steam injection.

Researchers have proposed various models to analyze the distribution of temperature and pressure in wells. Guyod [5] investigated the generation of temperature field and the static distribution of temperature field in the well. Moss and White [6] analyzed the temperature profile of long-term water-injection wells and Lesem et al. [7] investigated the temperature distribution along the well to better predict the flowing bottom-hole pressure. Ramey [8], for the first

Table 1: Modified Beggs-Brill flow pattern criteria.

Criteria	Flow pattern
$E_1 < 0.01, F_r < L_1$ or $E_1 > 0.01, F_r < L_2$	Segregated flow
$0.01 \le E_1 < 0.4, L_3 < F_r < L_1$ or $E_1 \ge 0.4, L_3 < F_r < L_4$	Intermittent flow
$L_2 < F_r < L_3$	Transition flow
$E_1 < 0.4, F_r \ge L_1$ or $E_1 \ge 0.4, F_r > L_4$	Distributed flow

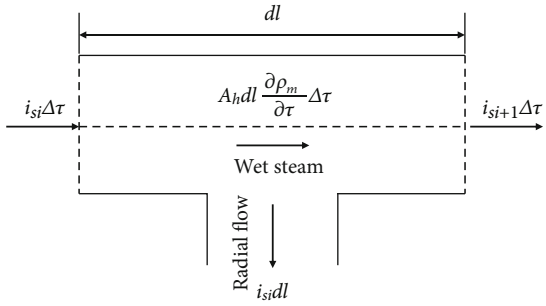

Figure 1: Schematic figure of mass conservation in an infinitesimal section.

time, quantitatively investigated the heat transfer between fluids and wells and proposed a simplified model to predict the temperature distribution in the well. Their model showed the influence of well depth and production time on the temperature distribution. Satter [9] improved previous heat transfer models to calculate the pressure distribution and heat loss by considering the injected steam as a function of well depth and temperature. Due to the neglection of the effect of pressure drawdown, the model was only applicable on shallow wells. Pacheco and Ali [10] proposed a new model by incorporating the effect of heat radiation, heat conduction and heat convection. This model analyzed the mechanics of wet and saturated steam flow along the well with temperature and pressure changes caused by friction. Galate and Mitchell [11] considered the effect of different flow regimes during the injection process. Their two-phase downward vertical flow pressure drop model was no longer limited by the assumption of homogeneous flow and showed higher accuracy in the predictions of temperature profiles. Livescu et al. [12] developed a fully-coupled thermal multiphase wellbore flow model to describe the distribution of pressure, temperature and phase composition along the well. The slip between different fluid phases and the heat losses were incorporated to the model and their model showed good agreement with the field data for both vertical and inclined wells. Dong et al. [13] developed a flow and heat transfer coupling model to investigate the multi-thermal fluid characteristics in horizontal wells. They considered the effect of fluid adsorption in perforated horizontal wellbore and proposed the effective heating length to measure the thermal efficiency. Their results showed that the multi-thermal fluids were in single-phase or two-phase conditions during the flowing process. The fluid viscosity had the most significant effect on flow behaviors and thermal characteristics of multi-thermal fluids.

In this paper, we develop a semi-analytical model to investigate the thermal properties and heat losses along the steam injection horizontal wellbore. The model is used to optimize steam injection process and provide steam injection plan for the horizontal injection well in Liaohe oilfield. The paper is organized as follows. In section 2, the semi-analytical model is derived in detail. In section 3, the model is first validated by the real field data to show the accuracy of the model. Then, a series of sensitivity analysis are performed to observe the effect of different parameters on wellbore pressure, wellbore temperature and steam quality. Finally, the model is used to optimize the steam injection plan of a horizontal injection well in Liaohe oilfield. In section 4, the conclusions are summarized to give a brief description of this work.

2. Methodology

2.1. Model Assumption. In the horizontal flow process, steam flows into the formation through the perforation holes, which leads to the decrease of the mass flow rate of steam. Under the condition of variant mass flow, the volumetric flow rate keeps decreasing due to the reduction of mass flow rate. The decrease of volumetric flow rate results in the acceleration loss. Therefore, the acceleration loss cannot be ignored when developing the model. Because of the pressure loss along the horizontal wellbore, the pressure is not evenly distributed at different perforations from the heel to the toe of horizontal wellbore. As a result, the flow rate in radial direction varies.

Based on the flow behavior mentioned above, the simplified cylindrical tube model is not available for the description of pressure and temperature profiles. A more accurate semi-analytical model is required to describe the steam injection process by incorporating the flow characteristics of steam. The assumptions are summarized below:

(1) The reservoir is homogeneous with the thickness of h

(2) The reservoir is infinite in the horizontal direction

(3) The heat transfer between wellbore and cement ring is one-dimensional steady heat transfer while the heat transfer between the cement ring and formation is one-dimensional unsteady heat transfer

(4) The heat dissipation of the collar is not considered and the heat transfer of steam in the horizontal direction is ignored

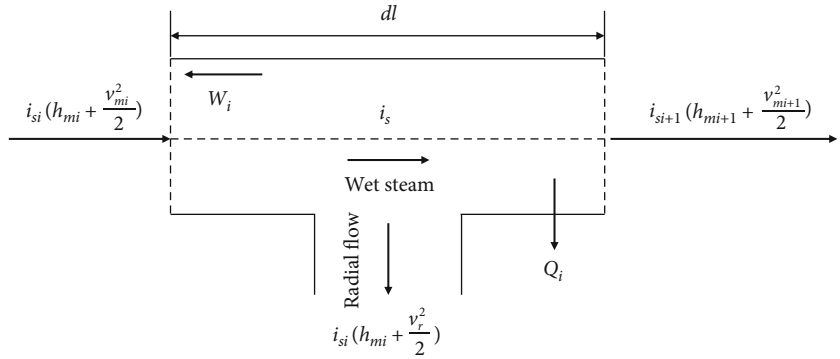

Figure 2: Schematic figure of energy conservation in an infinitesimal section.

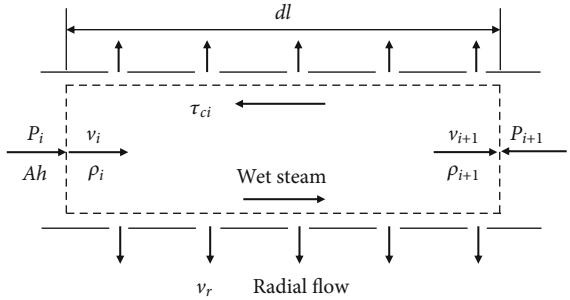

Figure 3: Schematic figure of momentum conservation in an infinitesimal section.

(5) The injection pressure, steam quality and mass flow rate at the heel of the horizontal well is kept constant and the flow of steam in horizontal wellbore is steady-state

2.2. Flow Pattern. Following the criteria proposed by Beggs and Brill [14], the gas-liquid two-phase flow in the horizontal well is divided into three categories: 1) segregated flow: the gas-liquid two-phase distribution is relatively uniform, including annular flow, wavy flow and stratified flow; 2) intermittent flow: the distribution of gas-liquid two-phase distribution is not uniform and sometimes has fluctuations, including plug flow and slug flow; 3) distributed flow: there exists a clear and smooth interface between the gas-liquid two-phase fluids, including bubble flow and mist flow.

After modification of the flow pattern map, we divide the map into four regions (segregated flow, intermittent flow, transition flow and distributed flow) with four straight lines (L_1, L_2, L_3, L_4), as shown in the equations below:

$$F_r = v_m^2/(gD) \tag{1}$$

$$L_1 = 316E_1^{0.302} \tag{2}$$

$$L_2 = 92.52 \times 10^{-5} E_1^{-2.4684} \tag{3}$$

$$L_3 = 0.10E_1^{-1.4156} \tag{4}$$

$$L_4 = 0.5E_1^{-6.733} \tag{5}$$

where F_r represents the Froude number, v_m denotes the average flow rate of two-phase flow, g is the gravitational constant, D means the diameter of the pipe and E_1 is the liquid holdup at the inlet. The criteria of the modified flow pattern map are summarized in Table 1.

2.3. Governing Equation

2.3.1. Mass Conservation Equation. We select an infinitesimal section from the horizontal wellbore and analyze the steam flow behaviors in this infinitesimal section. The schematic figure is shown in Figure 1.

According to the mass conservation principle [15, 16], the mass increment of the infinitesimal section is equal to the mass difference between the steam at the inlet and the steam at the outlet of the infinitesimal section. The mass conservation equation is shown as below:

$$i_{si}\Delta\tau - i_{si+1}\Delta\tau - i_{\text{is}}dl \cdot \Delta\tau = A_h dl \frac{\partial \rho_m}{\partial \tau}\Delta\tau \tag{6}$$

where i_{si} and i_{si+1} represent the mass of the steam at inlet and outlet of the infinitesimal section, respectively, $\Delta\tau$ is the time of flowing, A_h is the cross-section area of the infinitesimal section, ρ_m is the density of the steam in the infinitesimal section, i_{is} is the mass of the steam that penetrates into the formation. Divided by $dl \cdot \Delta\tau$ at both sides of equation (6), the equation can be written as

$$-A_h \frac{\partial \rho_m}{\partial \tau} = \frac{\partial i_{si}}{\partial l} + i_{\text{is}} \tag{7}$$

Based on the previous assumptions, the flow state of steam in the horizontal wellbore is steady-state. Therefore, we have

$$\frac{\partial \rho_m}{\partial \tau} = 0 \tag{8}$$

Substitute equation (8) into equation (7), we can get

$$\frac{\partial i_s}{\partial l} = -i_{\text{is}} \tag{9}$$

2.3.2. Energy Conservation Equation. Since the steam flows horizontally in a horizontal wellbore, the energy change

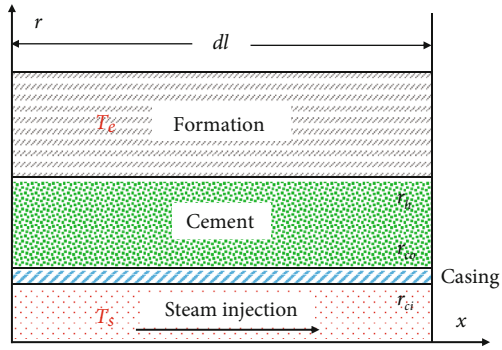

Figure 4: Schematic figure of heat transfer process between wellbore and formation.

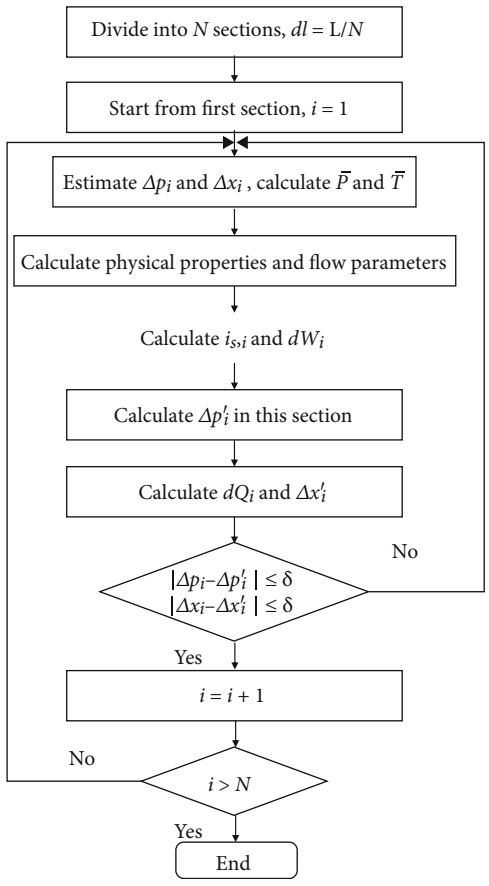

Figure 5: Workflow of model solvation.

caused by gravity can be ignored. The schematic figure is shown in Figure 2.

According to the energy conservation law [17], in unit time and unit length, the energy loss of steam in the infinitesimal section is equal to the sum of heat loss, friction loss and formation energy increment. The energy conservation equation is shown below:

$$\frac{dW}{dl} + i_{\text{is}}\left(h_m + \frac{v_r^2}{2}\right) + \frac{dQ}{dl} = -\frac{d}{dl}\left[i_s\left(h_m + \frac{v_m^2}{2}\right)\right] \quad (10)$$

where W is the work of friction, Q is the heat loss, l is the length of infinitesimal section, v_m is the horizontal flow rate of steam in the infinitesimal section, v_r is the flow rate of steam into formation and h_m is the enthalpy of steam mixture in the infinitesimal section. In equation (10), the effects of friction and variant mass flow are taken into consideration.

Based on the energy conservation equation, we can derive the equation of steam quality in the wellbore. Since the steam flow status in horizontal wellbore is gas-liquid two-phase flow, the enthalpy can be calculated as below:

$$h_m(x,t) = x \cdot h_s + (1-x)h_w \quad (11)$$

where h_s and h_w represent the enthalpy of steam and hot water, respectively, and x is the saturated steam quality. Take the derivative of h with respect to l and we have

$$\frac{dh_m}{dl} = h_s\frac{dx}{dl} + x\frac{dh_s}{dl} + \frac{dh_w}{dl}(1-x) - h_w\frac{dx}{dl} \quad (12)$$

After simplifying equation (12), we can get

$$\frac{dh_m}{dl} = (h_s - h_w)\frac{dx}{dl} + \left[x\frac{dh_s}{dl} + \left(1 - x\frac{dh_w}{dl}\right)\right] \quad (13)$$

Since the enthalpy of steam is the function of steam pressure, it can be written as $h = h(p)$. If we take the derivative of h with respect to l, we can get

$$\frac{dh}{dl} = \frac{dh}{dP}\frac{dP}{dl} \quad (14)$$

Substitute equation (14) into equation (13), we can get

$$\frac{dh_m}{dl} = (h_s - h_w)\frac{dx}{dl} + \frac{dh_w}{dP}\frac{dP}{dl} + \left(\frac{dh_s}{dP} - \frac{dh_w}{dP}\right)\frac{dP}{dl}x \quad (15)$$

Since $v_m = i_s/(\rho_m A_h)$, we have

$$\frac{d}{dl}\left(\frac{v_m^2}{2}\right) = v_m\frac{dv_m}{dl} = v_m\frac{d}{dl}\left(\frac{i_s}{\rho_m A_h}\right) = \frac{v_m}{\rho_m A_h}\frac{di_s}{dl} + \frac{v_m i_s}{A_h}d\left(\frac{1}{\rho_m}\right) \quad (16)$$

Generally, the gas volumetric flow rate is significantly higher than liquid volumetric flow rate. As a result, we can consider steam as ideal gas and apply the ideal gas law. The equation is shown below:

$$\frac{1}{\rho_m} = \frac{RT}{PM} \quad (17)$$

Take the derivative and simplify equation (17), we can get

$$d\left(\frac{1}{\rho_m}\right) = \frac{1}{\rho_m}\left(\frac{1}{T}\frac{dT}{dP} - \frac{1}{P}\right)dP \quad (18)$$

Table 2: Parameters of reservoir, wellbore and steam injection.

Parameter	Value	Unit	Parameter	Value	Unit
Reservoir thickness	287	m	Length of horizontal well	195.3	m
Reservoir temperature	18.8	˚C	Inner diameter of casing	0.0807	m
Reservoir pressure	2.38	MPa	Outer diameter of casing	0.0889	m
Permeability	1940	mD	Wellbore radius	0.12	MPa^{-1}
Porosity	0.32	—	Perforation density	12	m^{-1}
Water saturation	0.35	—	Perforation hole radius	0.0075	m
Oil viscosity	1366	mPa·s	Formation thermal conductivity	1.730	W/m/˚C
Oil volume factor	1.05	m^3/m^3	Cement thermal conductivity	0.933	W/m/˚C
Formation water volume factor	1.01	m^3/m^3	Steam pressure at the heel	5.13	MPa
Formation thermal diffusion coefficient	0.108	m^2/d	Steam temperature at the heel	336.5	˚C
Drainage area	29700	m^2	Steam injection rate	6.23	t/h

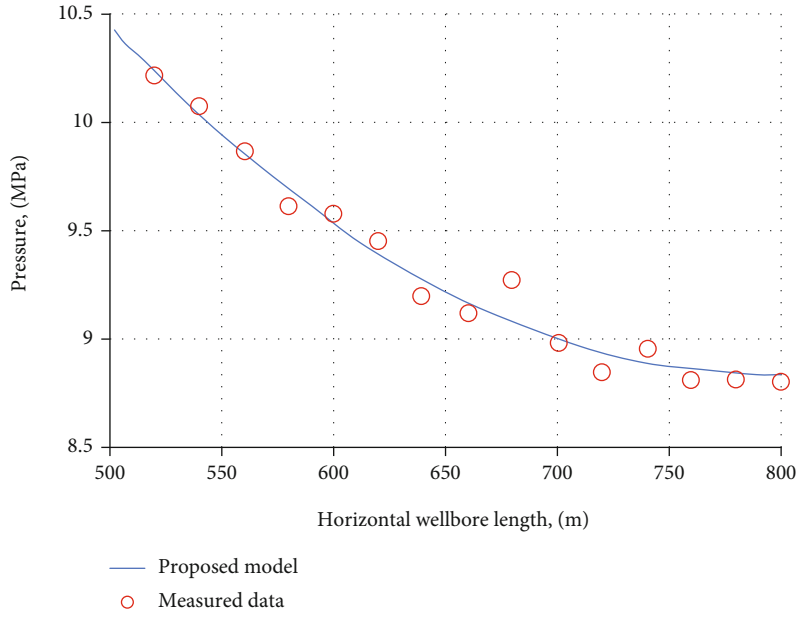

Figure 6: Steam pressure along the horizontal wellbore.

Substitute equation (18) into equation (16), we have

$$\frac{d}{dl}\left(\frac{v_m^2}{2}\right) = v_m\left[\frac{1}{\rho_m A_h}\frac{di_s}{dl} + \frac{i_s}{A}\frac{1}{\rho_m}\left(\frac{1}{T}\frac{dT}{dP} - \frac{1}{P}\right)\frac{dP}{dl}\right] \quad (19)$$

Then, we substitute equations (9), (15) and (19) into equation (10) and we can get

$$\begin{aligned}\frac{dQ}{dl} + \frac{dW}{dl} + \frac{di_s}{dl}\left(\frac{v_m^2 - v_r^2}{2}\right) &= -i_s\left\{\left[\frac{dx}{dl}(h_s - h_w) + \left(\frac{dh_s}{dP} - \frac{dh_w}{dP}\right)\frac{dP}{dl}x + \frac{dh_w}{dP}\frac{dP}{dl}\right]\right. \\ &\left. + v_m\left[\frac{i_s}{\rho_m A_h}\left(\frac{1}{T}\frac{dT}{dP} - \frac{1}{P}\right)\frac{dP}{dl} + \frac{1}{\rho_m A_h}\frac{di_s}{dl}\right]\right\}\end{aligned} \quad (20)$$

Let

$$\begin{aligned}N_1 &= i_s(h_s - h_w) \\ N_2 &= i_s\left(\frac{dh_s}{dP} - \frac{dh_w}{dP}\right)\frac{dP}{dl} \\ N_3 &= \frac{dQ}{dl} + \left(\frac{v_m^2 - v_r^2}{2}\right)\frac{di_s}{dl} + \frac{dW}{dl} + \frac{dh_w}{dP}\frac{dP}{dl}i_s \\ &\quad + v_m i_s\left[\frac{i_s}{\rho_m A_h}\left(\frac{1}{T}\frac{dT}{dP} - \frac{1}{P}\right)\frac{dP}{dl} + \frac{1}{\rho_m A_h}\frac{di_s}{dl}\right]\end{aligned} \quad (21)$$

Equation (20) can be simplified as below:

$$\frac{dx}{dl} + \frac{N_2}{N_1}x = -\frac{N_3}{N_1} \quad (22)$$

Given the location of calculation points, equation (22) is the first order ordinary differential equation with boundary

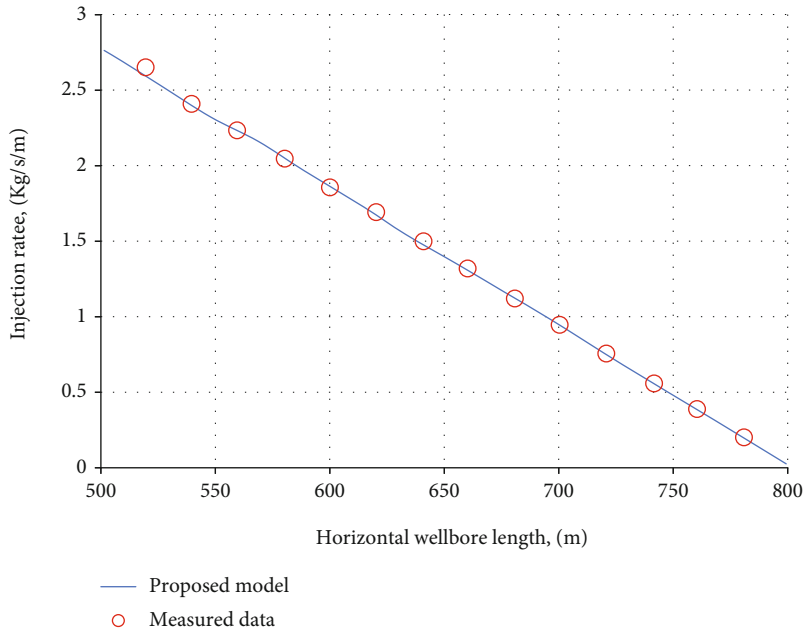

Figure 7: Steam injection rate along the horizontal wellbore.

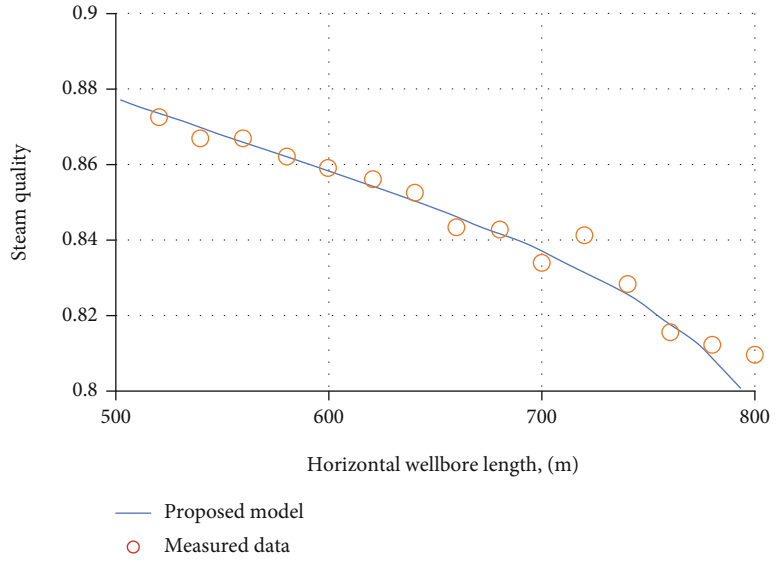

Figure 8: Steam quality along the horizontal wellbore.

conditions of $x|_{1=0} = x_0$ and $p|_{1=0} = p_0$ since N_1, N_2 and N_3 are constants. The distribution of steam quality in the wellbore can be obtained by solving equation (22). One particular solution of equation (22) is shown below:

$$x = \exp\left(-\frac{N_2}{N_1}l\right) \cdot \left[-\frac{N_3}{N_2}\exp\left(-\frac{N_2}{N_1}l\right) + x_0 + \frac{N_3}{N_2}\right] \quad (23)$$

2.3.3. Momentum Conservation Equation. The schematic figure of momentum conservation is shown in Figure 3. We can observe that, during flow process, the forces exerted on steam are mainly caused by the force generated by the pressure difference between the inlet and outlet of the infinitesimal section and the friction between the steam and the casing surface.

The momentum conservation equation is developed as follows:

$$(P_i - P_{i+1})A_h - \tau_c = d(v_m i_s) \quad (24)$$

Divided by the cross-section area at both sides of the equation, we can get

$$dP = -\left[\frac{d(v_m i_s)}{A_h} + \frac{A_h}{\tau_c}\right] = -\left(\frac{v_m di_s + i_s dv_m}{A_h} + \frac{\tau_c}{A_h}\right) \quad (25)$$

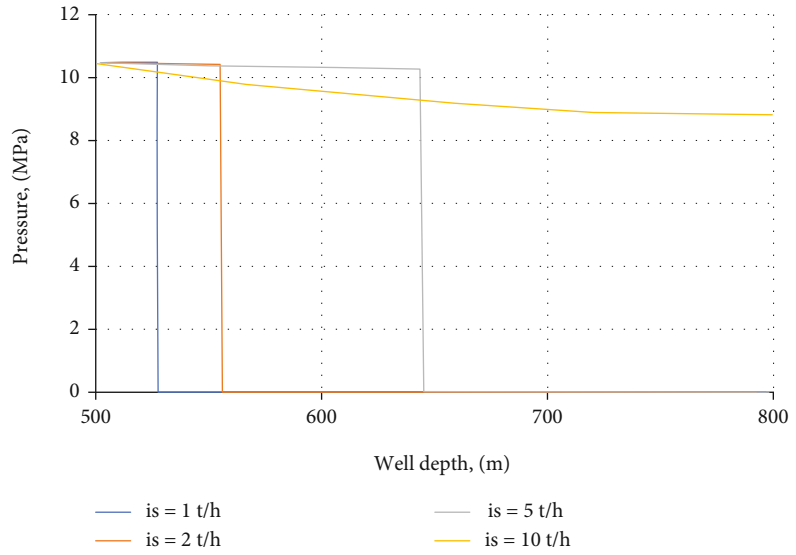

(a) steam injection rate

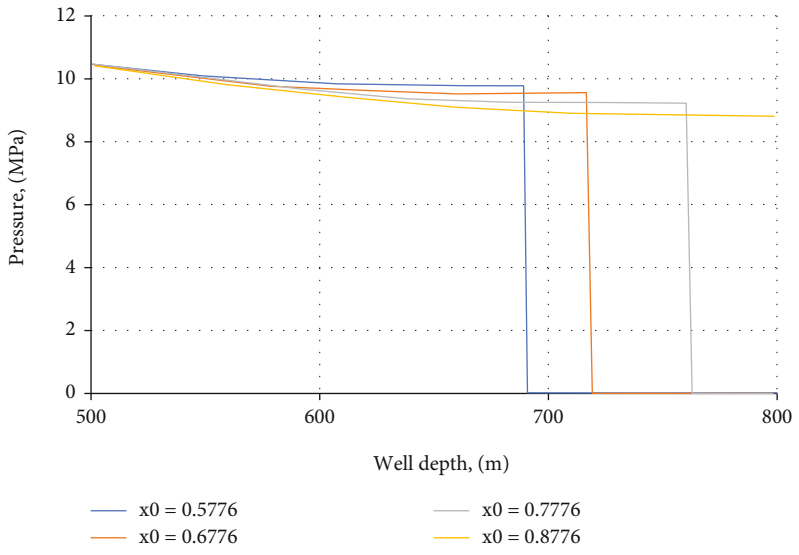

(b) steam quality at the heel

Figure 9: Continued.

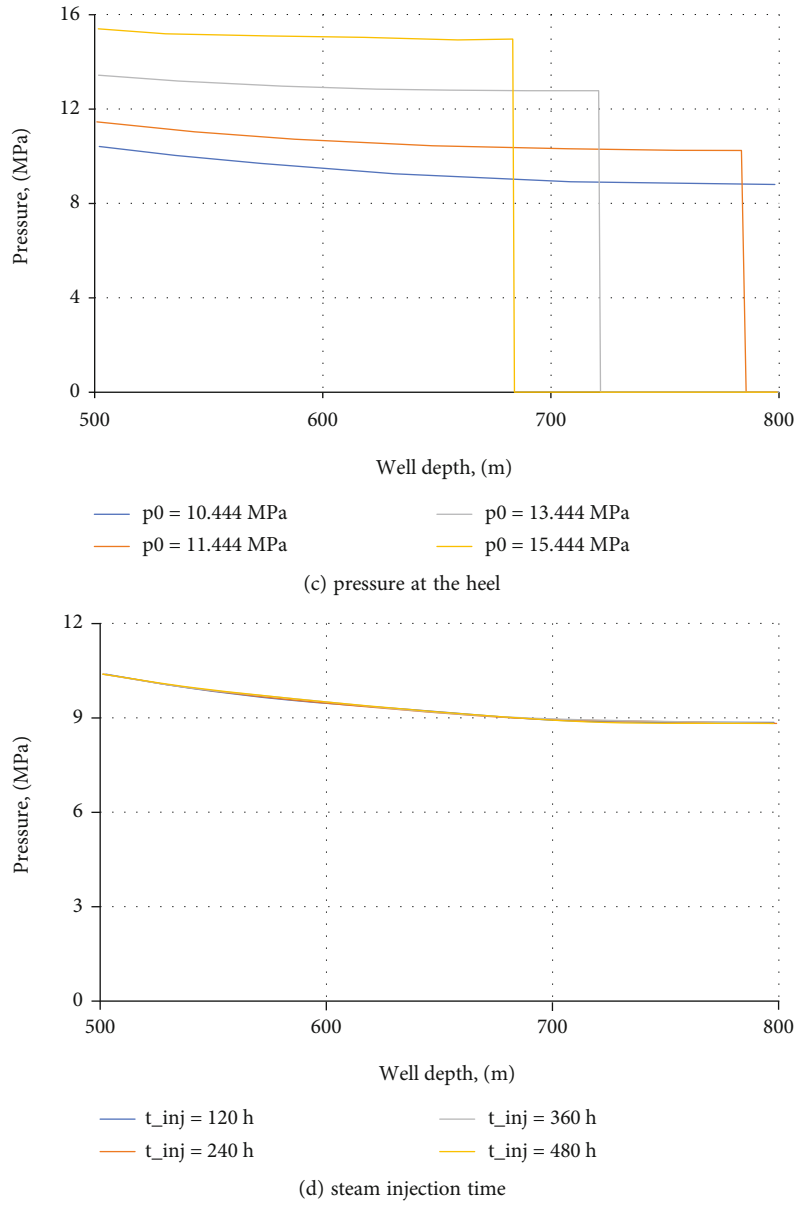

Figure 9: Effect of (a) steam injection rate, (b) steam quality at the heel, (c) pressure at the heel and (d) steam injection time on the distribution of pressure along the wellbore.

Substituting equation (18) into equation (25), we have

$$dP = -\frac{\tau_{ci} + 2v_m di_s}{A_h[(i_s v_m/A_h)((1/T)(dT/dP) - 1/P) + 1]} \quad (26)$$

Divided by dl, we obtain the model of the steam pressure in the horizontal wellbore:

$$\frac{dP}{dl} = -\frac{1}{A_h}\frac{2v_m(di_s/dl) + (\tau_c/dl)}{[1 + ((1/T)(dT/dP) - 1/P)(v_m i_s/A_h)]} \quad (27)$$

where τ_c is the friction between the steam and the inner surface of casing. The numerator of the right side of equation (27) describes the characteristics of variant mass flow in horizontal wellbore.

2.3.4. Other Parameters. In equation (10), the work of friction (W), velocity (v_m) and density (ρ_m) of steam mixture, the mass of the steam of the infinitesimal section (i_s) and heat losses (Q) have not been discussed. Next, we will show the equations to calculate these parameters.

During steam flow process, shear friction occurs between the steam and the inner surface of the casing. The direction of shear friction is opposite to the steam flow direction and therefore, the work of shear friction is negative. In unit time, the work of friction on the infinitesimal section of length dl

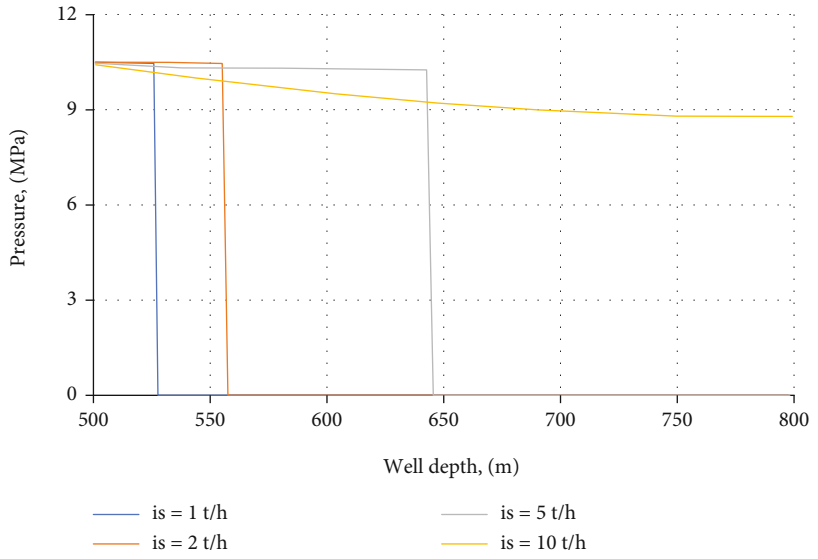

(a) steam injection rate

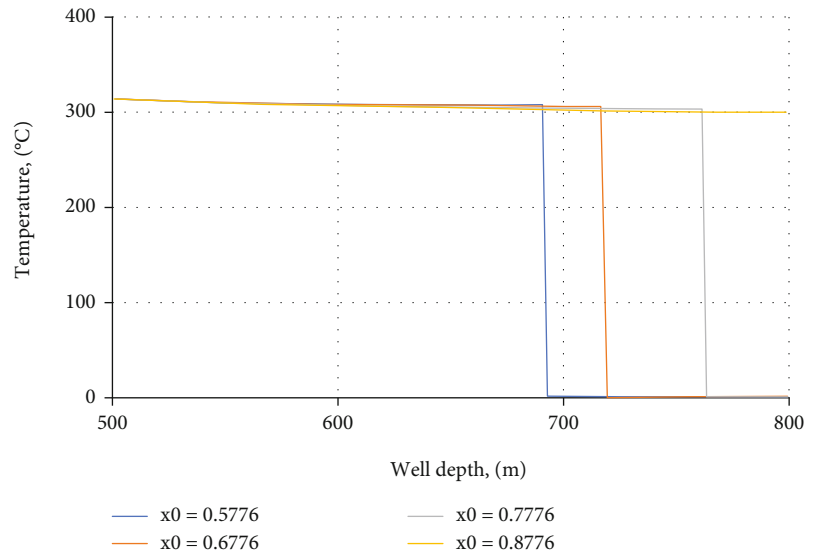

(b) steam quality at the heel

Figure 10: Continued.

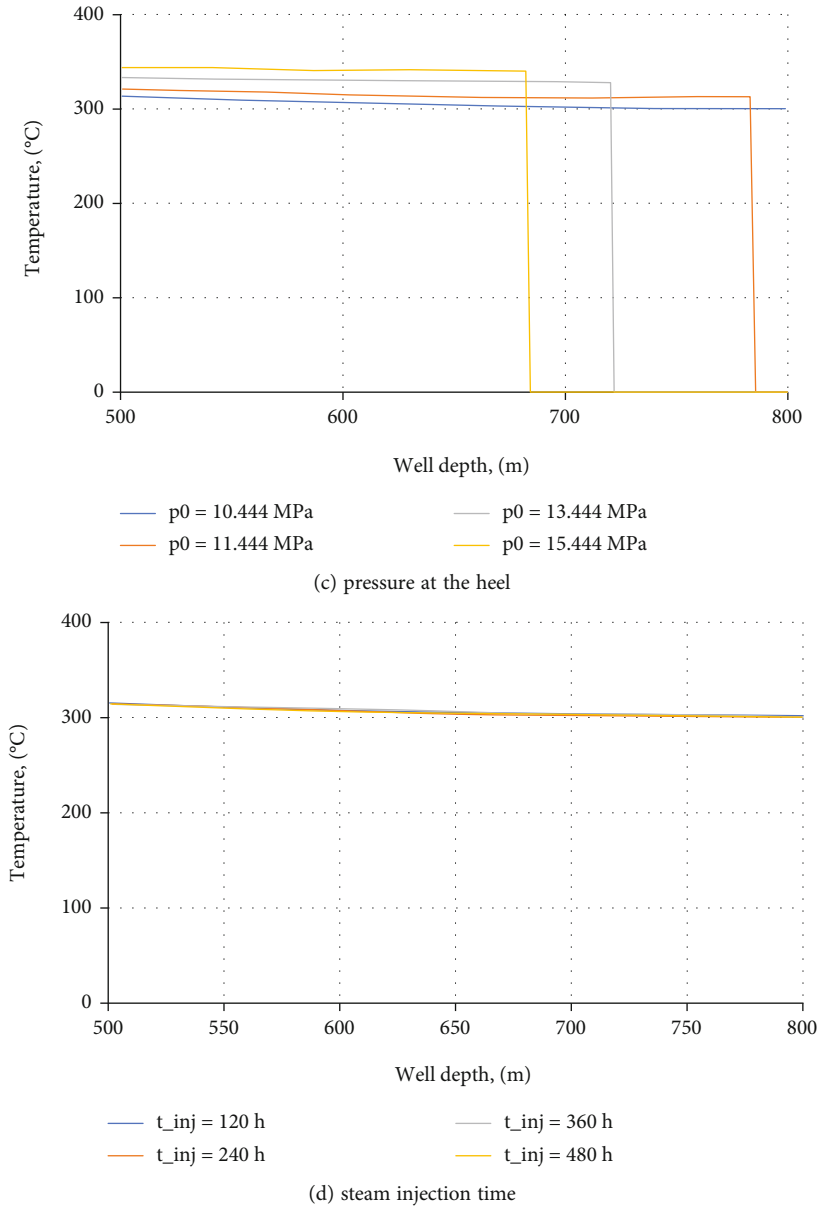

Figure 10: Effect of (a) steam injection rate, (b) steam quality at the heel, (c) pressure at the heel and (d) steam injection time on the distribution of temperature along the wellbore.

can be calculated as

$$dW = \frac{(\tau_c dl)}{dl/(v_{mi} + v_{mi+1}/2)} = \frac{\tau_c}{2}\frac{dl}{(v_{mi} + v_{mi+1})} \tag{28}$$

$$\tau_c = f_c \cdot \rho_m \cdot \frac{\pi D dl}{8}\left(\frac{v_{mi} + v_{mi+1}}{2}\right)^2 \tag{29}$$

where f_c is the friction coefficient between the steam and casing and D is the inner diameter of casing. In equation (29), the friction coefficient consists of two parts: the friction coefficient between the fluid and boundary surface and the friction coefficient between the steam and perforation holes. The friction coefficient between the fluid and boundary surface can be calculated by

$$f = \begin{cases} 64/R_e & R_e \le 2000 \\ \dfrac{0.3164}{\mathrm{Re}^{0.25}} & 3000 < R_e < 50.9/\varepsilon^{8/7} \\ \left\{-1.811g\left[\left(\dfrac{\varepsilon}{3.7D}\right)^{1.11} + \dfrac{6.9}{\mathrm{Re}}\right]\right\}^{-2} & 50.9/\varepsilon^{8/7} < R_e < (665 - 7651g\varepsilon)/\varepsilon \end{cases} \tag{30}$$

where R_e is the Reynolds number and ε is the absolute roughness of the wellbore. The friction coefficient between the steam and perforation holes is obtained using the

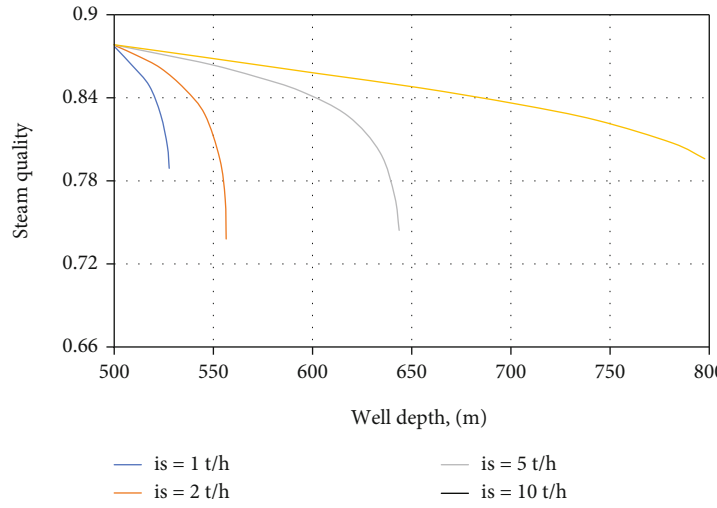

(a) steam injection rate

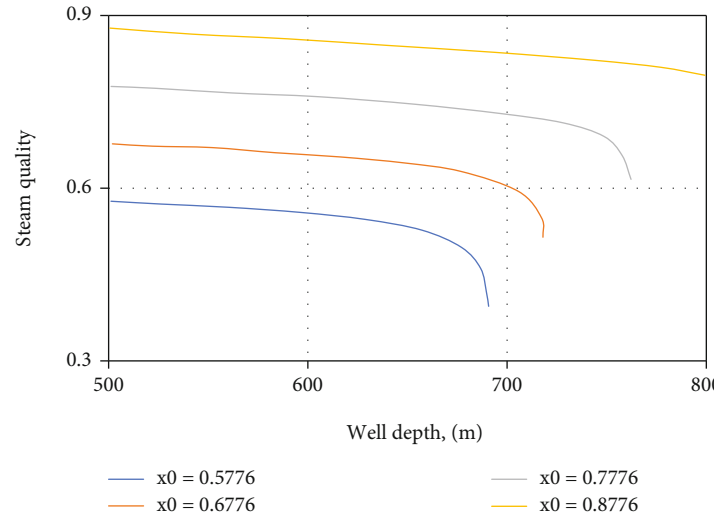

(b) steam quality at the heel

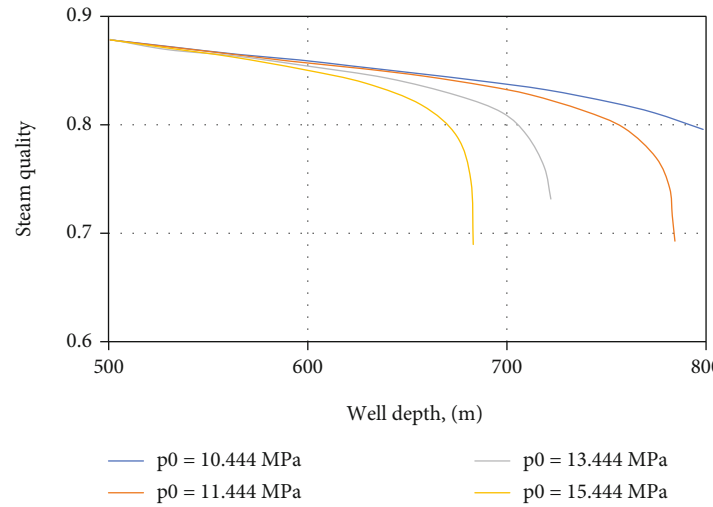

(c) pressure at the heel

Figure 11: Continued.

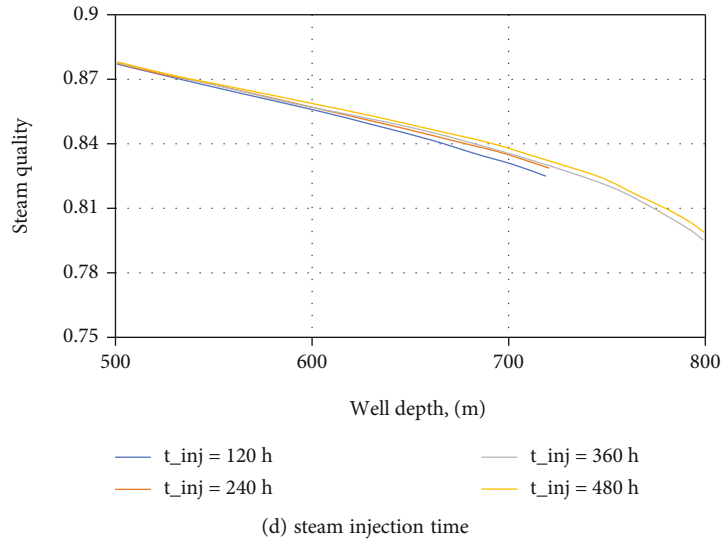

Figure 11: Effect of (a) steam injection rate, (b) steam quality at the heel, (c) pressure at the heel and (d) steam injection time on the distribution of steam quality along the wellbore.

equation shown below:

$$\sqrt{\frac{8}{f_p}} = 2.5 \ln\left(0.5\,\mathrm{Re}\sqrt{\frac{8}{f_p}}\right) + 1.744 - 7.0 \times \left(\frac{d_p}{D}\right) \times \left(\frac{n_p}{12}\right) - 3.75 \tag{31}$$

where d_p is the diameter of perforation hole and n_p is the perforation density. The total friction coefficient is the sum of these two friction coefficients.

The density of saturated steam is calculated based on the equation below:

$$\rho_m = \rho_w H_l + \rho_s (1 - H_l) \tag{32}$$

where ρ_m, ρ_w and ρ_s are the densities of saturated steam, water and dry steam, respectively, and H_l is the liquid holdup. The flow velocity of saturated steam is calculated using the equation below:

$$v_m = v_s + v_w = \frac{i_s x}{\rho_s A_h} + \frac{i_s (1 - x)}{\rho_w A_h} \tag{33}$$

The steam mass of the infinitesimal section of horizontal wellbore is calculated based on the equation below:

$$i_s = \rho_m \cdot I_s \cdot (P_s - P_i) \cdot J_1 \tag{34}$$

$$J_1 = \frac{2\pi\sqrt{K_h/K_v}K_v dl\alpha((K_{ro}/B_o\mu_o) + (K_{rw}/B_w\mu_w))}{\ln(r_{sh}/r_w) - 0.75 + S} \tag{35}$$

where I_s is the steam mass coefficient of unit length of formation, P_s is the steam injection pressure, P_i is the initial reservoir pressure and J_1 is the fluid productivity index.

Based on the assumption that the horizontal well is in an infinite formation, the heat capacity of the reservoir is infinite. As a result, the formation near the cement ring can be slowly heated by the steam while the formation away from the wellbore keeps the initial temperature. This heat transfer process is called unsteady-state heat transfer. The heat transfer process between the horizontal wellbore and the formation can be simplified into two parts: 1) the steady-state heat transfer between the wellbore and cement ring, 2) the unsteady-state heat transfer between the cement ring and formation. The schematic figure of the heat transfer process is shown in Figure 4.

For the infinitesimal section with length dl, the heat loss can be calculated by the equation shown below:

$$\frac{dQ}{dl} = \frac{T_s - T_e}{R} \tag{36}$$

where T_s and T_e are the temperatures of steam and initial formation, respectively. The material of casing is steel, which has a small thermal resistance that can be ignored. Therefore, the total thermal resistance can be calculated using the equations shown below:

$$R = \frac{1}{2\pi}\left[\frac{\ln(r_h/r_{co})}{\lambda_{cc}} + \frac{f(\tau)}{\lambda_c}\right] \tag{37}$$

$$f(\tau) = \ln\left(\frac{2\sqrt{\alpha\tau}}{r_h}\right) - 0.29 \tag{38}$$

where R is the total thermal resistance, r_h and r_{co} represent the external radius of cement ring and casing, respectively, λ_{cc} and λ_c denote the heat conductivity coefficients of cement ring and formation, respectively, α is the thermal diffusivity of formation. $f(\tau)$ shows the unsteady heat transfer property of formation.

2.4. Model Solvation. Due to the complexity of this model, it is hard to directly calculate the steam pressure, steam temperature and steam quality. As a result, the dual iteration

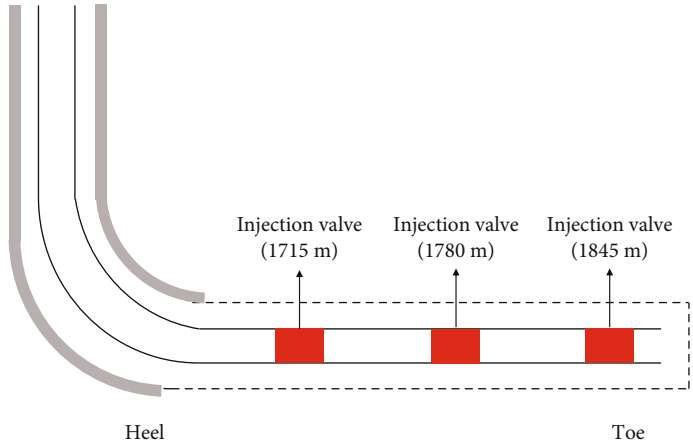

Figure 12: Schematic figure of Well XH27 in Liaohe oilfield.

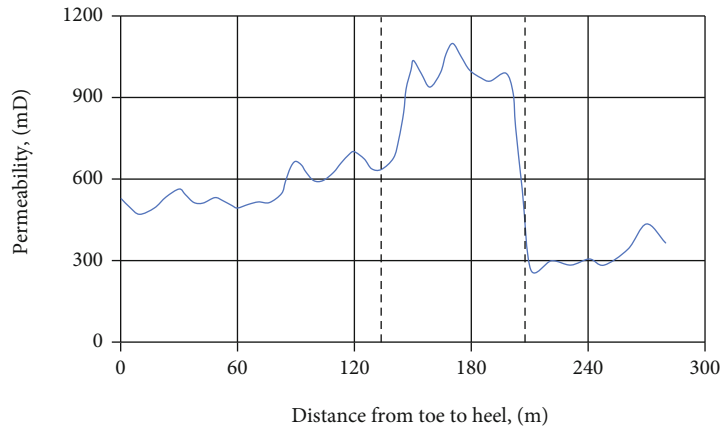

Figure 13: Distribution of permeability along the wellbore.

Table 3: Injection data of Well XH27.

Production location (m)	Starting injection date	End injection date	Steam injection pressure (MPa)	Daily injection amount (t)	Total injection amount (t)
1614~1817	05/14/2014	05/22/2014	11.8	141	1000.2

of pressure increment and steam quality increment is selected. The detailed procedures are shown below:

(1) The known data is the steam pressure, steam temperature, steam quality and mass flow rate at the heel of the horizontal well. Starting from the heel of the horizontal well, the horizontal well is divided into N sections and the length of each section is $dl = L/N$

(2) Estimate the change of steam quality (Δx) and pressure change (Δp) as the initial value in the iteration and calculate the average pressure and temperature of this section

(3) Apply the modified Beggs-Brill criteria to determine the physical properties and flow parameters of steam under the average pressure and temperature in step 2

(4) Use equation (34) to calculate the amount of steam penetrate into the formation and apply equation (28) to calculate the work of friction

(5) Use equation (27) to calculate the pressure gradient in this section and further obtain the pressure drop ($\Delta p'$) on length dl

(6) Apply equation (36) to calculate the heat loss in the section and use equation (23) to calculate the steam quality and steam quality change ($\Delta x'$) in the section

(7) Compare the values of $\Delta p'$ and $\Delta x'$ with the estimated Δp and Δx in step 2. If $|\Delta p - \Delta p'| \le \delta$ and $|\Delta x - \Delta x'| \le \delta$, the calculation results are considered reasonable. Otherwise, let $\Delta p = \Delta p'$ and $\Delta x = \Delta x'$ and return to step 2

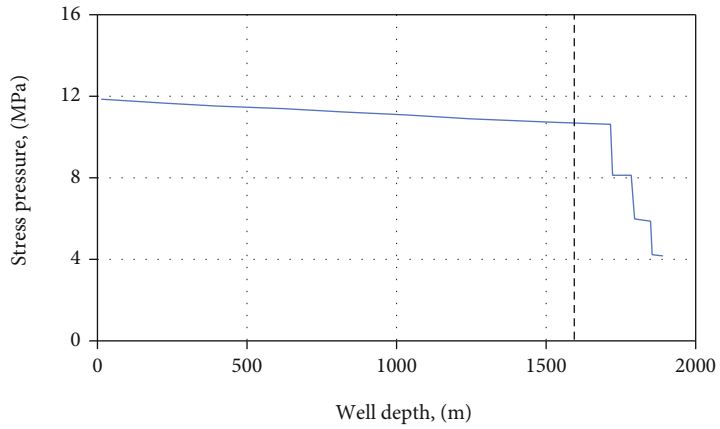

(a) steam pressure

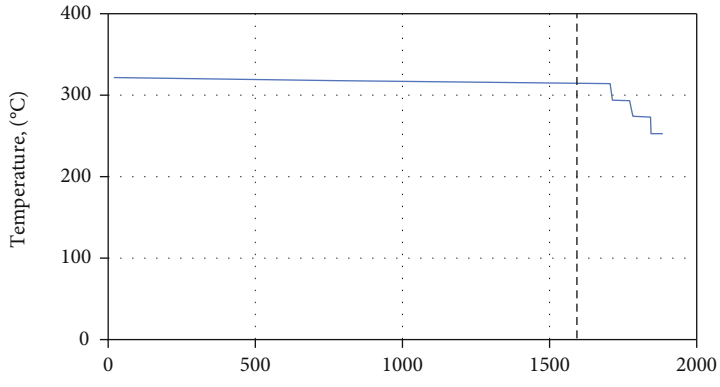

(b) steam temperature

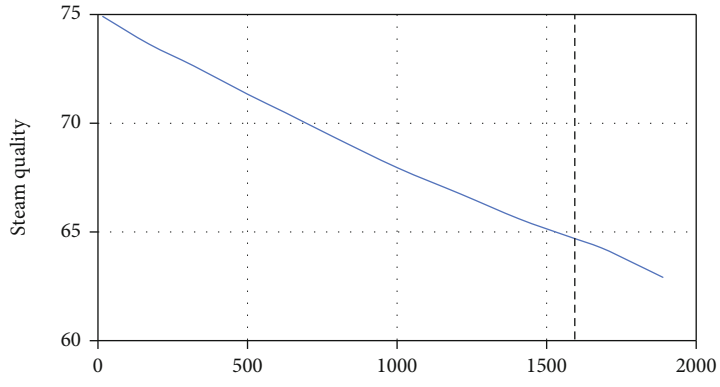

(c) steam quality

Figure 14: Continued.

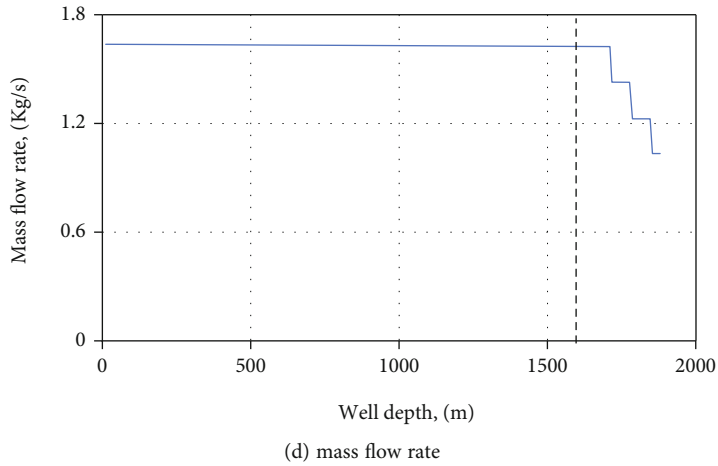

(d) mass flow rate

Figure 14: The (a) steam pressure, (b) steam temperature, (c) steam quality and (d) mass flow rate of steam along the wellbore of Well XH27.

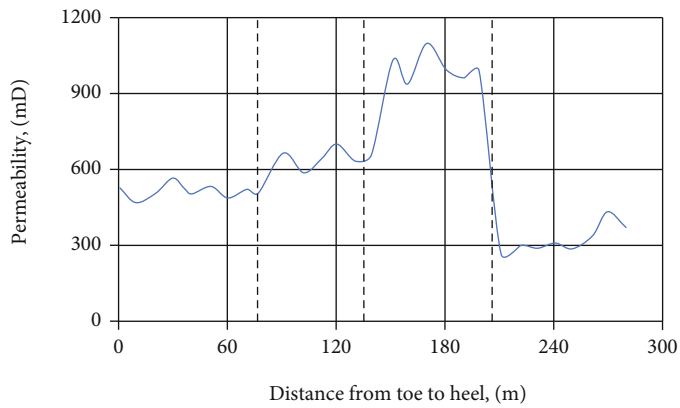

Figure 15: Distribution of permeability along the wellbore divided into 4 sections.

Table 4: Parameters of injection valves.

Injection valves	Location (m)	Size (mm)
New valve	1664	7.9
Valve I	1715	7.9
Valve II	1780	8.7
Valve III	1845	9.3

(8) Repeat steps 2 to 7 and calculate the steam pressure, steam temperature and steam quality in each section until all the sections are calculated

To be clear, the workflow is summarized in Figure 5.

3. Results and Analysis

3.1. Model Validation. To verify the accuracy of the model, we take the huff-and-puff horizontal well in a low-permeability heavy oil block in Liaohe oilfield as an example. The reservoir properties, well structure parameters and steam injection parameters are summarized in Table 2.

The steam pressure, steam injection rate and steam quality along the wellbore are calculated using the model and compared with field data. The results are shown in Figures 6, 7, 8. We can observe that the results of our model are consistent with the field data, indicating that our model can accurately predict the thermal properties of steam in horizontal wellbore.

3.2. Sensitivity Analysis. The distribution of steam pressure, steam temperature and steam quality in the horizontal well are influenced by many factors. Based on the established model, we investigate the effect of steam injection rate, steam quality at the heel, pressure at the heel and steam injection time on the distribution of steam pressure, steam temperature and steam quality in the horizontal well. The results are shown in Figures 9, 10 and 11.

In Figure 9(a), the steam pressure does not have significant effect on the steam injection rate. A high injection rate allows steam to flow further without completely cooling down to hot water. When the steam injection rate is less than 5 t/h, the steam becomes hot water at certain point in the wellbore. In Figure 9(b), we can observe that the steam quality does not have significant effect on steam pressure

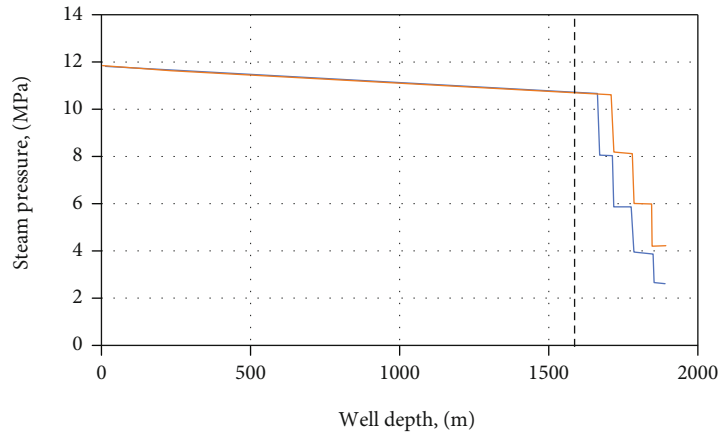

(a) steam pressure

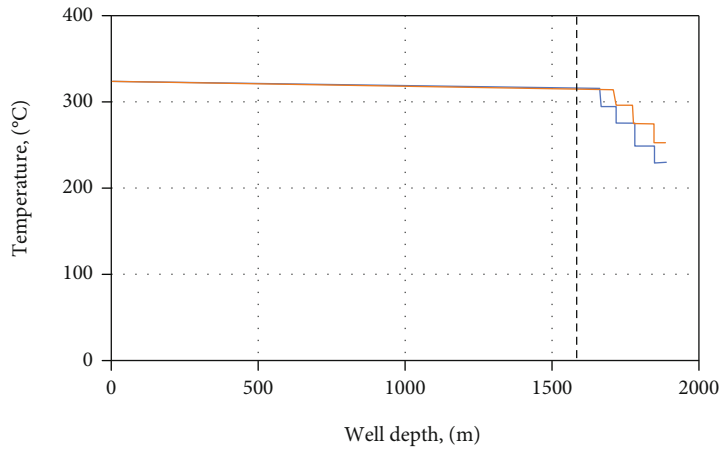

(b) steam temperature

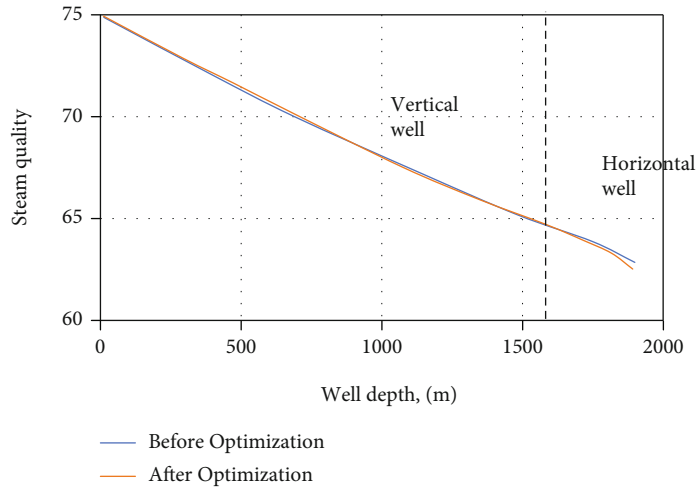

(c) steam quality

Figure 16: Continued.

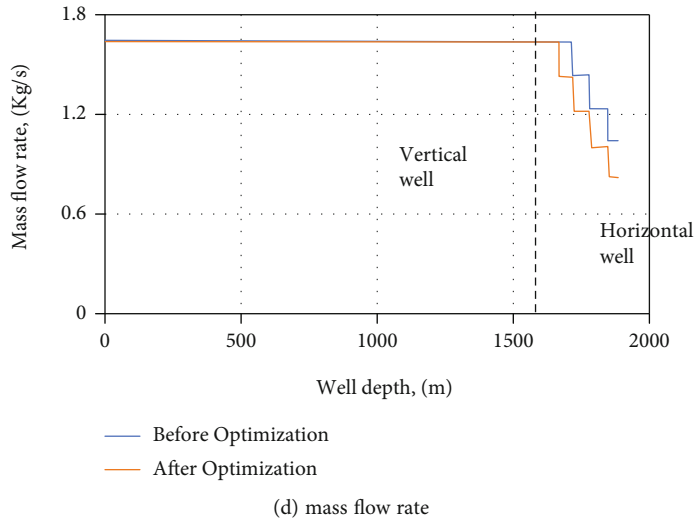

(d) mass flow rate

FIGURE 16: The (a) steam pressure, (b) steam temperature, (c) steam quality and (d) mass flow rate of steam along the wellbore of Well XH27 with optimized injection valves.

in the wellbore. When the steam is not completely cooled down to hot water, a small value of steam quality shows slightly higher steam pressure. In Figure 9(c), high steam pressure at the heel generally means a high steam pressure along the wellbore except the condition that the steam is totally cooled down to hot water. In addition, the extended distance of steam in the wellbore increases with the decrease of steam injection pressure. In Figure 9(d), we can observe that the steam injection time does not show any effect on steam pressure. The reason is that the steam is injected at constant pressure and rate and the increase of injection time only increase the total amount of steam injected to the wellbore.

In Figure 10(b), the steam quality at the heel does not have significant effect on steam temperature in the wellbore. The temperature decreases with the extension of the well. The temperature reduces to 0 sharply when the steam totally becomes hot water. In Figure 10(c), the steam temperature increases with the increase of steam pressure at the heel. The temperature slightly decreases with the extension of wellbore and reduces to 0 when no steam exists in the wellbore. In Figure 10(d), the steam injection time does not have significant effect on steam temperature because the injection time does not affect thermal properties of steam.

In Figure 11(a), the steam injection rate shows a significant effect on the steam quality. The increase of steam injection rate can largely increase the steam quality along the wellbore. With a low injection rate, the steam quality along the well decreases sharply. As a result, to ensure a high steam quality in the wellbore, we should inject steam at a relatively high rate. In Figure 11(b), a high steam quality at the heel shows a high steam quality in the whole wellbore. Regardless of the steam quality at the heel, the decline rate of steam quality along the wellbore is the same because the injection parameters and thermal conductivity are kept constant. In Figure 11(c), a high steam pressure at the heel shows a faster decrease of steam quality along the wellbore. In order to keep a high steam quality, the pressure at the heel should be maintained at a relatively low level. In Figure 11(d), the steam injection time does not have significant effect on the steam quality along the wellbore.

3.3. Field Case. Herein, we consider a horizontal steam injection well (Well XH27) in Liaohe oilfield and optimize the injection parameters of Well XH27 to improve the steam injection efficiency using our model. The schematic figure of this well is shown in Figure 12. As shown in the figure, initially there are three injection valves in the tubing located at the length of 1715, 1780 and 1845 m in Well XH27. The distribution of permeability along the wellbore is shown in Figure 13. The injection data of Well XH27 is summarized in Table 3.

Based on our model, we analyze the steam pressure, steam temperature, steam quality and mass flow rate of steam in Well XH27, as shown in Figure 14. We can observe that the steam pressure, steam temperature and steam quality increase with the increase of well depth. The increment is more significant in horizontal section compared with vertical section. In addition, the steam is continuously injected from the injection valves to the formation. The mass flow rate of steam keeps decreasing along the wellbore and the decreasing rate is affected by the formation permeability and parameters of injection valves. When the steam penetrates into the formation, due to its latent heat, the temperature of the region near the wellbore is the same as the temperature of steam while the temperature of the region away from the wellbore gradually reduces to the initial reservoir temperature.

To improve the injection efficiency, it is of great importance to optimize the parameters of injection valves, including the number of valves, the location of valves and the size of valves. Based on the distribution of formation permeability along the wellbore, we divide the horizontal wellbore into four sections, as shown in Figure 15. Accordingly, we add

one more injection valve at the length of 1664 m of the wellbore and the size of valves are determined by the injection flow rate. The parameters of injection valves are summarized in Table 4.

After adding one more injection valve and changing the size of valves, the steam pressure, steam temperature, steam quality and mass flow rate of steam in Well XH27 are shown in Figure 16. Compared with the initial condition, the optimized Well XH27 shows lower steam pressure, steam temperature and mass flow rate after adding an extra valve and the steam quality along the wellbore slightly decreases. The results indicate that more steam is injected to the formation to heat the region near the wellbore. Therefore, the viscosity of a larger range of heavy oil decreases and more oil will flow to the wellbore, which leads to a higher production rate.

4. Conclusions

(1) A semi-analytical model is proposed to investigate the physical and thermal properties of fluid in horizontal wellbore. Mass, energy and momentum conservation equations are considered in our model and the modified Beggs-Brill method is applied to determine the flow pattern of steam. The model can be used to calculate the steam pressure, steam temperature, steam quality and mass flow rate along the wellbore

(2) The semi-analytical model is validated with a horizontal steam injection well in Liaohe oilfield. The steam pressure, steam injection rate and steam quality calculated by the model show good consistency with field data, indicating that our model is accurate to predict the physical and thermal properties of fluid in horizontal wellbore

(3) Based on the sensitivity analysis, the steam quality along the wellbore is strongly affected by the steam pressure, steam injection rate and steam quality at the heel. Generally, the steam injection rate does not have significant effect on steam pressure, steam temperature and steam quality

(4) The semi-analytical model is used to optimize the injection valves in Well XH27 in Liaohe oilfield. Based on the formation permeability distribution, one extra injection valve is added and the sizes of injection valves are tuned according to the optimal steam injection rate. The optimized Well XH27 significantly increases the steam injection efficiency

Nomenclature

CCE: Constant composition expansion
A_h: Cross-section area
B: Formation volume factor
D: Diameter
E: Liquid holdup
f: Friction coefficient
F_r: Froude number
g: Gravitational constant
h: Enthalpy
i: Mass flow rate
J: Productivity index
K: Permeability
l: Length of infinitesimal section
M: Molecular mass
P: Pressure
Q: Heat loss
r: Radius
R: Ideal gas constant
R_e: Reynolds number
S: Skin factor
T: Temperature
v: Flow rate
W: Work of friction
x: Steam quality
α: Thermal diffusivity
ε: Absolute roughness
λ: Heat conductivity coefficient
μ: Viscosity
ρ: Density
τ: Flowing time.

Data Availability

Data available on request.

Conflicts of Interest

The authors declare that there is no conflict of interest regarding the publication of this paper.

Acknowledgments

This research was funded by Natural Science Foundation of Heilongjiang Province of China (Grant No. LH2021E014).

References

[1] W. Chunsheng, Z. Yan, L. Zejun, and Y. Fuxiang, "Heat transfer simulation and thermal efficiency analysis of new vertical heating furnace," *Case Studies in Thermal Engineering*, vol. 13, article 100414, 2019.

[2] G. Zhu, S. Zhang, Q. Liu et al., "Distribution and treatment of harmful gas from heavy oil production in the Liaohe oilfield, Northeast China," *Petroleum Science*, vol. 7, no. 3, pp. 422–427, 2010.

[3] D. A. N. G. Ben, Z. H. A. O. Hong, W. E. I. Heming, and D. U. N. Tiejun, "Thermal simulation testing study and influence factor analysis of asphaltene precipitation in the condition of viscous oil thermal recovery-a case study of viscous oil pools in the Xinglongtai oil reservoirs of Du-84 block, Shuguang-1 district, Liaohe oilfield," *Petroleum Geology & Experiment*, vol. 25, no. 3, pp. 305–309, 2003.

[4] Y. Bao, J. Y. Wang, and I. D. Gates, "History match of the Liaohe oil field SAGD operation-a vertical-horizontal well reservoir production machine," in *In SPE Heavy Oil Conference Canada. OnePetro*, Calgary, Alberta, Canada, 2012.

[5] H. C. Guyod, "Temperature well-logging heat conduction," *Oil Wkly.;(United States)*, vol. 123, p. BM-IC-7414, 1946.

[6] J. T. Moss and P. D. White, "How to calculate temperature profiles in a water-injection well," *Oil and Gas J*, vol. 57, no. 11, p. 174, 1959.

[7] L. B. Lesem, F. Greytok, F. Marotta, and J. J. McKetta, "A method of calculating the distribution of temperature in flowing gas wells," *Transactions of the AIME*, vol. 210, no. 1, pp. 169–176, 1957.

[8] H. Ramey Jr., "Wellbore heat transmission," *Journal of Petroleum Technology*, vol. 14, no. 4, pp. 427–435, 1962.

[9] A. Satter, "Heat losses during flow of steam down a wellbore," *Journal of Petroleum Technology*, vol. 17, no. 7, pp. 845–851, 1965.

[10] E. F. Pacheco and S. M. Ali, "Wellbore heat losses and pressure drop in steam injection," *Journal of Petroleum Technology*, vol. 24, no. 2, pp. 139–144, 1972.

[11] J. W. Galate and R. F. Mitchell, "Downward Two-Phase Flow Effects in Heat-Loss and Pressure-Drop Modeling of Steam Injection Wells," in *In SPE California Regional Meeting. OnePetro*, Bakersfield, California, 1985.

[12] S. Livescu, L. J. Durlofsky, K. Aziz, and J.-C. Ginestra, "Application of a New Fully-Coupled Thermal Multiphase Wellbore Flow Model," in *In SPE Symposium on Improved Oil Recovery. OnePetro*, Tulsa, Oklahoma, USA, 2008.

[13] X. Dong, H. Liu, Z. Zhang, and C. Wang, "The flow and heat transfer characteristics of multi-thermal fluid in horizontal wellbore coupled with flow in heavy oil reservoirs," *Journal of Petroleum Science and Engineering*, vol. 122, pp. 56–68, 2014.

[14] D. H. Beggs and J. P. Brill, "A study of two-phase flow in inclined pipes," *Journal of Petroleum Technology*, vol. 25, no. 5, pp. 607–617, 1973.

[15] W. Hao, G. Zhao, and S. Ma, "Failure behavior of horseshoe-shaped tunnel in hard rock under high stress: phenomenon and mechanisms," *Transactions of Nonferrous Metals Society of China*, vol. 32, no. 2, pp. 639–656, 2022.

[16] Z. Sun, S. Wang, H. Xiong, K. Wu, and J. Shi, "Optimal nanocone geometry for water flow," *AICHE Journal*, vol. 68, no. 3, article e17543, 2022.

[17] Z. Sun, B. Huang, K. Wu et al., "Nanoconfined methane density over pressure and temperature: wettability effect," *Journal of Natural Gas Science and Engineering*, vol. 99, p. 104426, 2022.